Available online at www.sciencedirect.com
ScienceDirect
Journal of Power Sources 159 (2006) 336–339
JOURNAL OF POWER SOURCES
www.elsevier.com/locate/jpowsour

Short communication

$NbSb_2$ as an anode material for Li-ion batteries

M. Anji Reddy, U.V. Varadaraju *

Materials Science Research Centre, Department of Chemistry, Indian Institute of Technology Madras, Chennai 600 036, India

Available online 8 June 2006

Abstract

Polycrystalline samples of $NbSb_2$ have been synthesized and studied as anode material for lithium-ion batteries. The reaction mechanism of lithium with $NbSb_2$ is investigated by ex situ XRD and cyclic voltammogram studies. Li_3Sb and Nb are formed during first discharge and during charge lithium is extracted from Li_3Sb. The first cycle discharge capacity is 420 mA hg^{-1} and first cycle charge capacity is 315 mA hg^{-1}.

Keywords: $NbSb_2$; Anode; Lithium-ion batteries

1. Introduction

The choice of anode material in state-of-the-art lithium-ion cells is graphite. However, the theoretical capacity is limited to 372 mA hg^{-1} corresponding to the intercalation of one Li per six carbon atoms. Several binary lithium alloys (e.g. Li–Al, Li–Si, Li–Sn, and Li–Sb) having high energy density (both volumetric and gravimetric) were investigated as possible replacement to graphite [1]. For example, 4.4Li atoms can react per Sn and deliver a specific capacity of 991 mA hg^{-1}. However, these alloys showed poor capacity retention during cycling [1]. This is attributed to the fragmentation of particles due to differences in volume caused by compositional changes that occur during cycling. As the particles fragment, they become electrically isolated, and hence the capacity of the cell decreases. In order to improve the cycling performance of these alloy systems, several strategies have been proposed.

Some of the compounds that are studied intensively in the literature include Cu_6Sn_5 [2], $CoSb_3$ [3,4] and Sn–Fe–C [5–7]. Lithium can be topochemically inserted into Cu_6Sn_5 within the voltage range 1.2–0.2 V. In the case of $CoSb_3$, Co and Li_3Sb are formed during discharge and during charge Co reacts with Sb to form $CoSb_x$. $FeSn_2$ reacts completely with Li during discharge and during charge, structure regains partly. In the light of these strategies several compounds have been studied, viz. InSb [8,9]; MnSb, Mn_2Sb [10]; Cu_2Sb [11]; Ag_3Sb [12]; $CoFe_3Sb_{12}$ [13]; $CrSb_2$ [14]; Mn–Sn–C [15].

The objective of this work is centered in developing this aspect in a structurally different material $NbSb_2$, in which clusters of niobium are possible.

2. Experimental

Stoichiometric amounts of high purity (99.9%) Nb and Sb were ground, pressed into pellet and placed in carbon coated quartz tube. The quartz tube is then evacuated and sealed at a vacuum of 10^{-5} Torr. This quartz ampoule is heated slowly at the rate of 1 °C per min to 750 °C and kept for 5 days.

Structural characterization of the sample is done by powder X-ray diffraction (XRD) (Rich Seifert P3000, Germany, Cu $K\alpha_1$ radiation). Unit cell parameters are calculated using AUTOX program.

For electrochemical studies, electrodes were fabricated by mixing active material, acetylene black (Denka Singapore Pvt. Ltd.) and polyvinylidene fluoride (PVDF) in the weight ratios 75:15:10. For comparison, electrodes were fabricated without acetylene black by keeping PVDF weight ratio as constant. The slurry prepared by using *N*-methyl-2-pyrrolidinone is spread on a stainless steel foil and dried in an oven at 100 °C for 12 h. Swagelok cells were fabricated in an argon filled glove box (mBraun, Germany, <5 ppm H_2O) with lithium foil as anode, Teklon (Anatek, USA) as separator and 1 M $LiPF_6$ in 1:1 EC + DMC (Chiel industries Ltd., Korea) as the electrolyte. Charge–discharge cycling of the cells is carried out in galvanostatic mode at *C*/5 and *C*/10 rate at room temperature by using Arbin battery cycling unit (BT2000, USA). GITT (galvanostatic intermittent titration technique) is performed at *C*/20 rate

* Corresponding author. Tel.: +91 44 2257 4215.
E-mail address: varada@iitm.ac.in (U.V. Varadaraju).

0378-7753/$ – see front matter © 2006 Published by Elsevier B.V.
doi:10.1016/j.jpowsour.2006.04.052

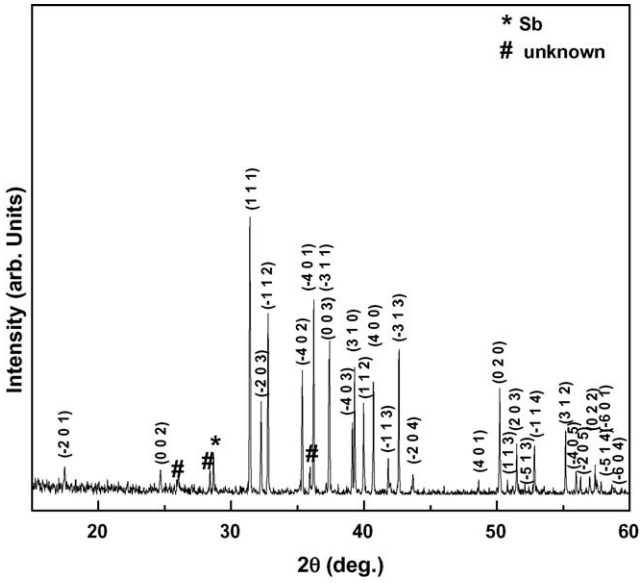

Fig. 1. Powder X-ray diffraction patterns of $NbSb_2$.

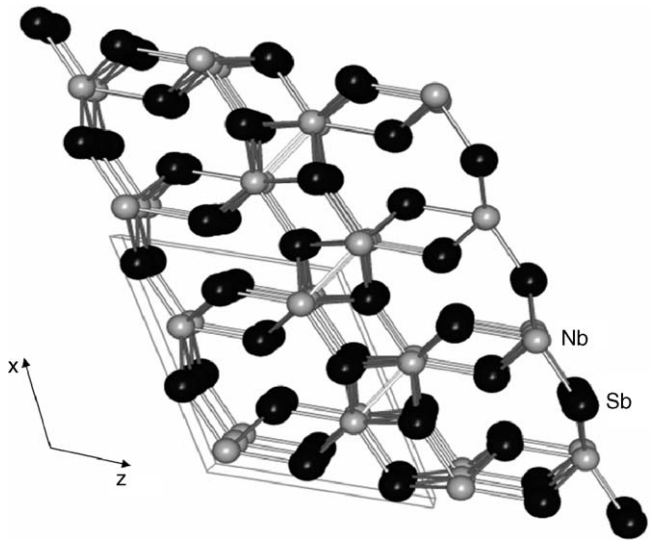

Fig. 2. Crystal structure of $NbSb_2$. Gray circles: Nb; black circles: Sb.

by passing current for 30 min and allowing for equilibration for 30 min. Cyclic voltammetry is carried out on an Autolab PGSTAT 30 instrument with $NbSb_2$ as working electrode and lithium foil as both counter and reference electrodes. At various lithiated and delithated states, the cells were disassembled inside the glove box. The electrodes were covered with a mylar film and ex situ XRD patterns were obtained.

3. Results and discussion

The powder XRD patterns shown in Fig. 1 are indexed according to the monoclinic $NbSb_2$ (JCPDS file no. 18-902) indicating the formation of well crystalline phase. A peak at 28.65° 2θ is due to Sb (indicated with *) and three minor unknown peaks are observed at 26°, 28.42°, 35.58° 2θ (indicated with #). The lattice parameters calculated by least squares fitting are $a = 10.24(2)$ Å, $b = 3.61(2)$ Å and $c = 8.34(2)$ Å.

The crystal structure of $NbSb_2$ [16] is shown in Fig. 2. Structure of $NbSb_2$ is described elsewhere [17]. $NbSb_2$ forms a structure of $OsGe_2$ type, with the Nb atoms surrounded by eight Sb atoms in the form of a bi-capped trigonal prism, and one Nb–Nb bond exists as a consequence of fusion of two $NbSb_8$ prisms via a common rectangular face.

GITT studies are carried out on $NbSb_2$ to determine the quasi-equilibrium open circuit potential at various reduction levels on both the electrodes, with (15%) and without acetylene black. The GITT curves of $NbSb_2$ electrodes are shown in Fig. 3. In the case of pure $NbSb_2$, the electrochemical reaction is found to be incomplete and meager 1.5Li reacted on complete discharge to 0.05 V. Hence, for further electrochemical studies, 15% acetylene black containing electrodes are used.

The voltage–capacity-composition profiles of 15% acetylene black containing $NbSb_2$ electrode cycled galvanostatically at *C*/5 rate are shown in Fig. 4. During initial discharge, the voltage drops from the open circuit voltage of 2.6 to 0.9 V. A plateau at ~0.8 V is attributed to the intercalation of lithium into acetylene black and reaction of Sb which is present as an impurity. The plateau at ~0.35 V corresponds to the reaction of $NbSb_2$. This lower discharge potential of $NbSb_2$ compared to the other Sb based intermetallic compounds like $CrSb_2$ [4] and $CoSb_3$ [3] in the first cycle is attributed to the lower reduction potential of Nb. The first discharge capacity of Li/$NbSb_2$ cell cycled at *C*/5 rate after subtracting the capacity due to the acetylene black is ~420 mA hg^{-1} which corresponds to the reaction of ~5.3Li. The first charge capacity is 315 mA hg^{-1} corresponds to the extraction of 4Li. The faradaic efficiency of the first cycle is about 75%.

Theoretical specific capacity of $NbSb_2$ from the following equation is calculated to be 480 mA hg^{-1} corresponding to 6Li:

$$NbSb_2 + 6Li \rightarrow 2Li_3Sb + Nb$$

The reaction mechanism of Li with $NbSb_2$ during the first cycle is followed by taking ex situ XRD patterns of the electrodes at

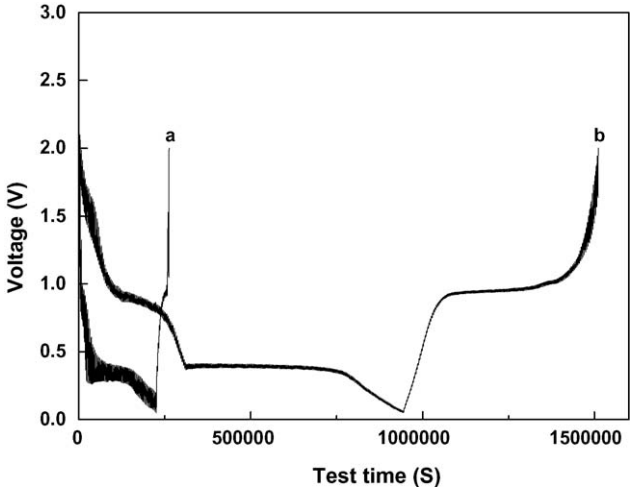

Fig. 3. GITT curve of Li/$NbSb_2$ (a) without acetylene black and (b) with acetylene black (15%) in the voltage range 0.05–2 V.

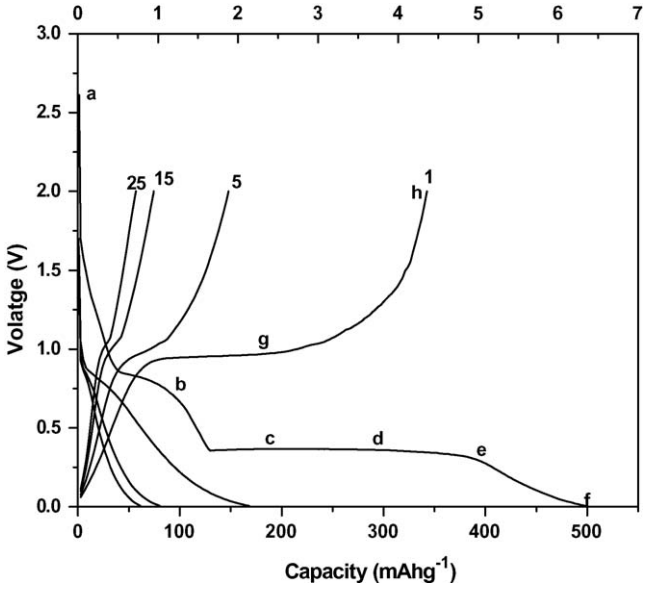

Fig. 4. Capacity–voltage-composition profiles of Li/$NbSb_2$ cell cycled galvanostatically at *C*/5 rate (1*C* corresponds reaction of 1Li in 1 h).

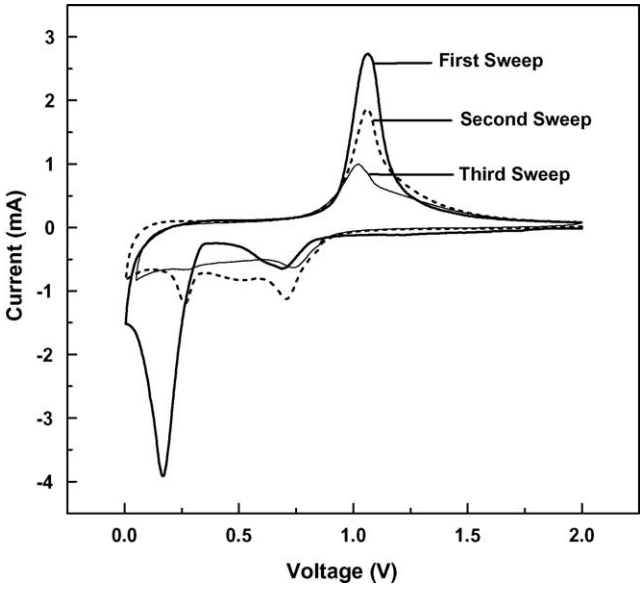

Fig. 6. Cyclic voltammogram of Li/$NbSb_2$ cell for first three scans.

various voltages. The XRD patterns shown in Fig. 5 are taken at the steps indicated in Fig. 4. There is no significant change in the XRD pattern (b) up to 0.7 V, which is the end of the first plateau. This indicates that the initial plateau is due to the intercalation of Li into acetylene black. Further reaction of Li down to 0.005 V is accompanied by the formation of Li_3Sb, which is evident from the XRD patterns of corresponding electrodes (c–f). The XRD pattern of fully charged electrode (h) shows the disappearance of Li_3Sb indicating the extraction of Li from Li_3Sb.

The cyclic voltammograms of $NbSb_2$ for the first three scans are shown in Fig. 6. In the first scan, the potential was swept in the cathodic direction down to 0.005 V and then in anodic direction to 2.0 V with a scan rate of 0.1 mV s^{-1}. During cathodic sweep a small peak is observed at 0.7 V. This is attributed to the intercalation of Li into graphite and reaction of Li with Sb. A strong peak is observed at 0.2 V corresponding to the destruction of the lattice and leading to the formation of Li_3Sb and Nb. In anodic sweep a strong peak at around 1 V is due to the extraction of Li from Li_3Sb. In the second scan, the initial peak at 0.7 V is attributed to the reaction of Sb and peak at around 0.2 V is due to the reaction of $NbSb_2$, either remained unreacted in the first cycle or formed during first charge. On cycling the areas under cathodic and anodic regions decrease and this indicates poor reversibility. Based on the discharge/charge, ex situ XRD

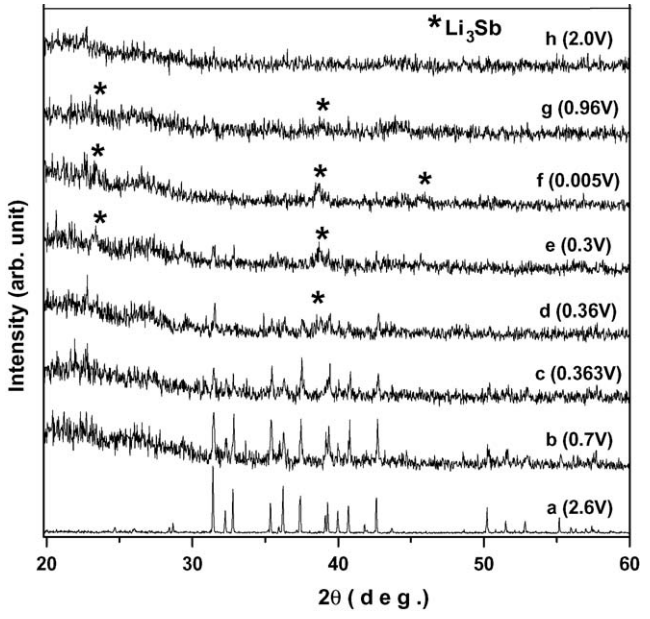

Fig. 5. Ex situ XRD patterns of Li/$NbSb_2$ cell at various lithiated and delithiated states.

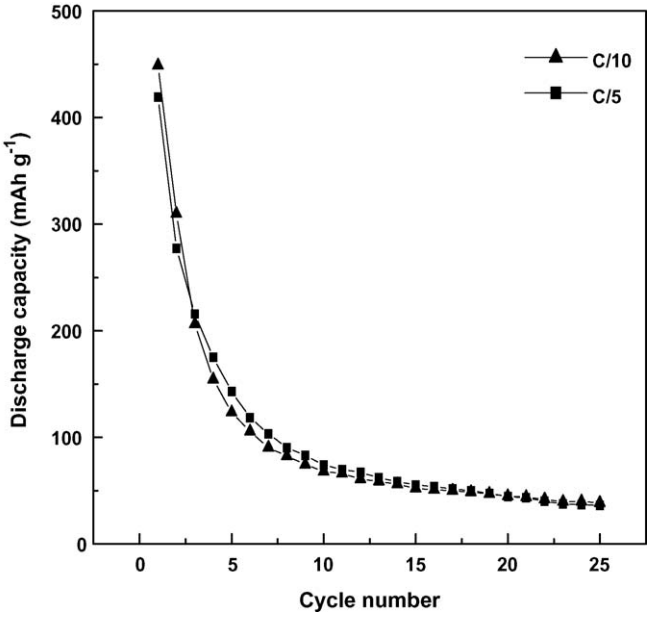

Fig. 7. Discharge capacity vs. cycle number of Li/$NbSb_2$ cells cycled in voltage window 0.005–2 V at *C*/5 and *C*/10 rate.

and cyclic voltammograms studies, the following mechanism is proposed for the first cycle:

- During discharge:

$$NbSb_2 + 5.4Li \rightarrow 1.8Li_3Sb + 0.9Nb + 0.1NbSb_2$$

- During charge:

$$1.8Li_3Sb \rightarrow 1.4Sb + 4.2Li + 0.4Li_3Sb$$

The cycling behavior of the $NbSb_2$ cycled at *C*/5 and *C*/10 rates are shown in Fig. 7. The initial discharge capacity of the electrode cycled at *C*/10 rate is more compared to that of cycled at *C*/5 rate. However, on further cycling both the capacities fade to a constant value.

4. Conclusions

Electrochemical studies on $NbSb_2$ are carried out for the first time. GITT studies show that $NbSb_2$ with 15% acetylene black is more reactive than the pure compound. The XRD patterns taken at the end of each step of discharge and charge indicate the formation and disappearance of Li_3Sb, respectively. The retention of capacity is found to be poor during cycling. This can probably be improved by reducing the particle size.

References

[1] J. Wang, I.D. Raisrtick, R.A. Huggins, J. Electrochem. Soc. 133 (1986) 457.
[2] K.D. Kepler, J.T. Vaughey, M.M. Thackeray, Electrochem. Solid State Lett. 2 (1999) 307.
[3] R. Alcantara, F.J. Fernandez-madrigal, P. Lavela, J.L. Tirado, J.-C. Jumas, J. Oliver-Fourcade, J. Mater. Chem. 9 (1999) 2517.
[4] J.-M. Tarascon, M. Morcrette, L. Dupont, Y. Chabre, C. Payen, D. Larcher, V. Pralong, J. Electrochem. Soc. 150 (6) (2003) A732.
[5] O. Mao, R.A. Dunlap, J.R. Dahn, J. Electrochem. Soc. 146 (1999) 405.
[6] O. Mao, J.R. Dahn, J. Electrochem. Soc. 146 (1999) 414.
[7] O. Mao, J.R. Dahn, J. Electrochem. Soc. 146 (1999) 423.
[8] J.T. Vaughey, J. O'Hara, M.M. Thackeray, Electrochem. Solid State Lett. 3 (1) (2000) 13.
[9] K.C. Hewitt, L.Y. Beaulieu, J.R. Dahn, J. Electrochem. Soc. 148 (5) (2001) A402.
[10] L.M.L. Fransson, J.T. Vaughey, K. Edström, M.M. Thackeray, J. Electrochem. Soc. 150 (1) (2003) A86.
[11] L.M.L. Fransson, J.T. Vaughey, R. Benedek, K. Edstrom, J.O. Thomas, M.M. Thackery, Electrochem. Commun. 3 (2001) 317.
[12] J.T. Vaughey, L. Fransson, H.A. Swinger, K. Edström, M.M. Thackeray, J. Power sources 1–5 (2003) 5266.
[13] L.J. Zhang, X.B. Zhao, X.B. Jiang, C.P. Lv, G.S. Cao, J. Power Sources 94 (2001) 92.
[14] F.J. Fernández-Madrigal, P. Lavela, C. Pérez-Vicente, J.L. Tirado, J. Electroanal. Chem. 501 (2001) 205.
[15] L.Y. Beaulieu, J.R. Dahn, J. Electrochem. Soc. 147 (9) (2000) 3237.
[16] A. Rehr, S.M. Kauzlarich, Acta Crystallogr., Sect. C: Cryst. Struct. Commun. 50 (1994) 1177.
[17] S. Derakhshan, K.M. Kleinke, E. Dashjav, H. Kleinke, Chem. Commun. (2004) 2428.